

# Neptunium incorporation into uranyl compounds that form as alteration products of spent nuclear fuel: Implications for geologic repository performance

By Peter C. Burns<sup>1,\*</sup>, Kathryn M. Deely<sup>1</sup> and Suntharalingam Skanthakumar<sup>2</sup>

<sup>1</sup> Department of Civil Engineering and Geological Sciences, University of Notre Dame, 156 Fitzpatrick Hall, Notre Dame, Indiana 46556-0767, USA

<sup>2</sup> Chemistry Division, Argonne National Laboratory, Argonne, Illinois 60439, USA

(Received June 23, 2003; accepted in revised form January 4, 2004)

*Neptunium / Nuclear waste / Uranophane /  
Compreignacite / Meta-schoepite*

**Summary.** Alteration of spent nuclear fuel in a geological repository under oxidizing conditions is likely to result in abundant uranyl compounds. Incorporation of radionuclides into the uranyl alteration phases may significantly reduce their mobility, thereby impacting repository performance. The following compounds have been synthesized from solutions containing from ~ 10 to 500 ppm  $\text{Np}^{5+}$ : meta-schoepite,  $\text{UO}_3 \cdot 2\text{H}_2\text{O}$ ; Na-compreignacite,  $\text{Na}_2[(\text{UO}_2)_3\text{O}_2(\text{OH})_3]_2(\text{H}_2\text{O})_7$ ; uranophane,  $\text{Ca}(\text{UO}_2)_2(\text{SiO}_3\text{OH})_2(\text{H}_2\text{O})_5$ ; and  $\beta\text{-(UO}_2\text{)(OH)}_2$ . The structures of each involve sheets of uranyl polyhedra; the interlayers contain cations and  $\text{H}_2\text{O}$  groups in Na-compreignacite and uranophane, only  $\text{H}_2\text{O}$  in meta-schoepite, and  $\beta\text{-(UO}_2\text{)(OH)}_2$  does not contain interlayer constituents. Synthesized powders were characterized by X-ray powder diffractometry, and were analyzed by ICP-AES (U, Na, Ca) and ICP-MS (Np). Aliquots of the powders were washed in 0.5 M acetic acid to remove sorbed Np prior to analysis. The powders of meta-schoepite and  $\beta\text{-(UO}_2\text{)(OH)}_2$  contained at most a few ppm  $\text{Np}^{5+}$ . In contrast, powders of Na-compreignacite and uranophane contained  $\text{Np}^{5+}$  in proportion to the  $\text{Np}^{5+}$  concentration in the mother solution, and powders of each containing more than 400 ppm  $\text{Np}^{5+}$  (of total Np + U) were obtained. Incorporation of  $\text{Np}^{5+}$  into uranyl compounds that form in a geological repository appears possible, and may impact the mobility of Np.

## 1. Introduction

Safe disposal of nuclear waste in a geological repository such as Yucca Mountain, Nevada, USA involves many unique scientific and engineering challenges because the repository must retain radionuclides with vastly different chemical characters for thousands of years. Most of the radioactive material to be housed in the proposed repository at Yucca Mountain is spent nuclear fuel derived from commercial reactors. Studies of natural analogues of geological repositories, which emphasize the mineral uraninite,

$\text{UO}_{2+x}$  (an analogue for  $\text{UO}_2$  in commercial spent nuclear fuel) [1, 2], as well as laboratory-scale studies of alteration of both  $\text{UO}_2$  and commercial spent fuel [3–8], indicate that spent fuel is unstable under the moist, oxidizing conditions expected in the proposed repository at Yucca Mountain. Once containers are breached, alteration of the spent fuel is likely to be rapid, leading to the formation of uranyl ( $\text{U}^{6+}$ ) phases that may persist for thousands of years [9].

The long half-life of  $^{237}\text{Np}$  ( $2.14 \times 10^6$  years) and potential high mobility of  $\text{Np}^{5+}$  in chemically oxidizing groundwater make it one of the most important radionuclides for the long-term performance of the proposed repository at Yucca Mountain. Uranyl compounds formed due to alteration of spent fuel may incorporate various radionuclides, including Np, released from spent fuel [10–18]. Such incorporation could have a profound impact upon the mobility of radionuclides. Burns *et al.* [12] predicted, on the basis of crystal-chemical arguments, that  $\text{Np}^{5+}$  may be incorporated into uranyl compounds. Buck *et al.* [10] reported 550 ppm Np in dehydrated schoepite formed as an alteration product of spent fuel, although these results were preliminary. The final report of the Yucca Mountain Total Systems Performance Assessment Peer Review Panel [19] emphasized the need for systematic evaluation of the extent of incorporation of  $^{237}\text{Np}$  into uranyl compounds that may form in Yucca Mountain. Such studies are essential to assess the importance of this mechanism of radionuclide retention on repository performance.

This manuscript reports initial results of a study concerning incorporation of  $\text{Np}^{5+}$  into selected uranyl compounds. The extent of  $\text{Np}^{5+}$  incorporation into powders with a variety of structures and chemistry grown between 70 and 100 °C, from solutions containing from about 10 to 500 ppm  $\text{Np}^{5+}$ , is reported.

## 2. Alteration of spent nuclear fuel and $\text{UO}_2$ under simulated Yucca Mountain conditions

Alteration of  $\text{UO}_2$ , the mineral uraninite, under oxidizing conditions results in a suite of complex alteration products dominated by uranyl compounds [20]. Mineralogical studies

\* Author for correspondence (E-mail: pburns@nd.edu).

have established the paragenetic sequences of uranyl minerals that result from alteration of  $\text{UO}_2$  [1, 2, 20, 21]. Several laboratory studies have been conducted to simulate the behavior of spent fuel and  $\text{UO}_2$  under conditions expected in Yucca Mountain.

Finch *et al.* [5] and Wronkiewicz *et al.* [3, 4] studied the alteration of spent fuel and  $\text{UO}_2$ , respectively, in the presence of slowly dripping groundwater. The intent was to simulate conditions in Yucca Mountain where groundwater could drip onto spent fuel following canister failure. Finch *et al.* [5] examined the alteration products that formed after groundwater dripped onto the fuel for six years at 90 °C. The experiments used two pressurized-water-reactor fuels, ATM103 and ATM106, with corresponding burn-up histories of  $\sim 30$  MWd/kg-U and  $\sim 45$  MWd/kg-U, respectively. The groundwater used was from well J-13 at the Yucca Mountain site, and was reacted with crushed Tonopah Springs tuff at 90 °C for 80 days. The resulting water, designated EJ-13, contains more Na and Si than J-13 water, with Na and Si concentrations of 46.5 and 34.4  $\mu\text{g}/\text{mL}$ , respectively [3]. Four different experiments involved injection rates of  $\sim 0.15$  and  $\sim 1.5$  mL of per week of EJ-13 water. Alteration of the spent fuel in each experiment was observed after six years, with uranyl compounds being the main alteration phases. These included meta-schoepite,  $\text{UO}_3 \cdot 2\text{H}_2\text{O}$ ; dehydrated schoepite,  $(\text{UO}_2)\text{O}_{0.25-x}(\text{OH})_{1.5+2x}$ ; tentatively the Na analogue of compreignacite (hereafter designated Na-compreignacite),  $\text{Na}_2[(\text{UO}_2)_3\text{O}_2(\text{OH})_3]_2(\text{H}_2\text{O})_7$ ; soddyite,  $(\text{UO}_2)_2\text{SiO}_4(\text{H}_2\text{O})_2$ ;  $\beta$ -uranophane,  $\text{Ca}(\text{UO}_2)_2(\text{SiO}_3\text{OH})_2(\text{H}_2\text{O})_5$ ; Na-boltwoodite,  $(\text{Na}, \text{K})(\text{UO}_2)(\text{SiO}_3\text{OH})(\text{H}_2\text{O})_{1.5}$ ; and a Cs-Ba-Mo uranate,  $(\text{Cs}, \text{Ba})(\text{UO}_2)_5(\text{MoO}_6)(\text{OH})_6(\text{H}_2\text{O})_n$  [5].

Wronkiewicz *et al.* [3, 4] examined  $\text{UO}_2$  that was under dripping EJ-13 water at 90 °C for more than 10 years, with water injection rates of 0.075 mL every 3.5 days or 0.0375 mL every seven days. The alteration products present up to 10 years after the onset of the experiment were characterized. Uranyl phases identified were: meta-schoepite; dehydrated schoepite; compreignacite,  $\text{K}_2[(\text{UO}_2)_3\text{O}_2(\text{OH})_3]_2(\text{H}_2\text{O})_7$ ; becquerelite,  $\text{Ca}[(\text{UO}_2)_6\text{O}_4(\text{OH})_6](\text{H}_2\text{O})_8$ ; uranophane,  $\text{Ca}(\text{UO}_2)_2(\text{SiO}_3\text{OH})_2(\text{H}_2\text{O})_5$ ; boltwoodite,  $\text{K}(\text{UO}_2)(\text{SiO}_3\text{OH})(\text{H}_2\text{O})_{1.5}$ ; Na-boltwoodite; and sklodowskite,  $\text{Mg}[(\text{UO}_2)(\text{SiO}_3\text{OH})_2(\text{H}_2\text{O})_6]$ . Wronkiewicz *et al.* [4] found that the paragenetic sequence of uranyl phases that formed throughout the experiments involved initially uranyl oxide hydrates, followed by uranyl silicates. This sequence is similar to those observed in natural analogue studies, such as the Nopal I deposit, Peña Blanca District, Chihuahua, Mexico [2].

### 3. Selection of uranyl compounds for study

Uranyl compounds selected for our initial study of  $\text{Np}^{5+}$  incorporation could be synthesized with high yields and purity, and are relevant to the expected chemical environment of the proposed repository. Synthesis of most uranyl compounds in high yields and purity in a single synthesis reaction is difficult, and optimization of synthesis techniques required  $\sim 100$  experiments prior to studies of  $\text{Np}^{5+}$  incorporation. The compounds selected

were uranophane, Na-compreignacite, meta-schoepite and  $\beta$ - $(\text{UO}_2)(\text{OH})_2$ . These phases provide considerable structural diversity. Uranophane, Na-compreignacite and meta-schoepite were reported as alteration products of spent fuel or  $\text{UO}_2$  under simulated Yucca Mountain conditions using EJ-13 water [4, 5].

### 4. Structures of uranyl compounds selected for study

The structures of  $\text{U}^{6+}$  minerals and synthetic compounds almost invariably involve approximately linear  $(\text{UO}_2)^{2+}$  uranyl ions that are further coordinated by from four to six ligands arranged at the equatorial vertices of square, pentagonal and hexagonal bipyramids. Due to the uneven distribution of bond-valences in uranyl polyhedra [22], polymerization of uranyl polyhedra, either with other uranyl polyhedra or with other cation-centered polyhedra of high valence, most often results in sheets, which are contained in  $\sim 80\%$  of known uranyl mineral structures. Burns *et al.* [23] and Burns [24] developed a structural hierarchy for uranyl minerals and synthetic compounds based upon the polymerization of polyhedra of higher bond-valence, and reviewed the details of the structures of uranyl compounds. Structures were grouped according to the connectivity of their structural units: finite clusters, chains, sheets and frameworks of polyhedra of higher bond-valence.

Burns *et al.* [23] developed the concept of a sheet anion-topology for structures containing uranyl polyhedra. In brief, the sheet anion-topology is the projection onto a plane of the topology of the two-or-more connected anions within the sheet, and in general represents the close-packing of anions within the sheet. The significance of this approach is that apparently unrelated structures often have the same underlying sheet anion-topology. Burns *et al.* [12] used this approach to predict incorporation mechanisms of various transuranics, including  $\text{Np}^{5+}$ , into the structures of uranyl compounds.

#### 4.1 Uranophane

The structure of uranophane [25] consists of sheets of uranyl pentagonal bipyramids and silicate tetrahedra, with  $\text{Ca}^{2+}$  cations and  $\text{H}_2\text{O}$  groups located in the interlayer (Fig. 1a). The uranyl pentagonal bipyramids involve nearly linear  $(\text{UO}_2)^{2+}$  uranyl ions (designated Ur) that are coordinated by five O atoms arranged at the equatorial vertices of the bipyramids, which are capped by the  $\text{O}_{\text{Ur}}$  atoms. Uranyl pentagonal bipyramids share equatorial edges, forming chains one polyhedron wide. Each uranyl pentagonal bipyramid shares one equatorial edge with a silicate tetrahedron, such that tetrahedra alternate on opposite sides of the chain along the chain length. The resulting chains are linked by the sharing of vertices between silicate tetrahedra and uranyl polyhedra, resulting in a sheet (Fig. 1b). Only three of the ligands of the silicate tetrahedra are linked to uranyl polyhedra; the remaining is an OH group that extends towards the interlayer.

#### 4.2 Na-compreignacite

The structure of Na-compreignacite has not been reported, but X-ray powder diffraction data indicates that it is

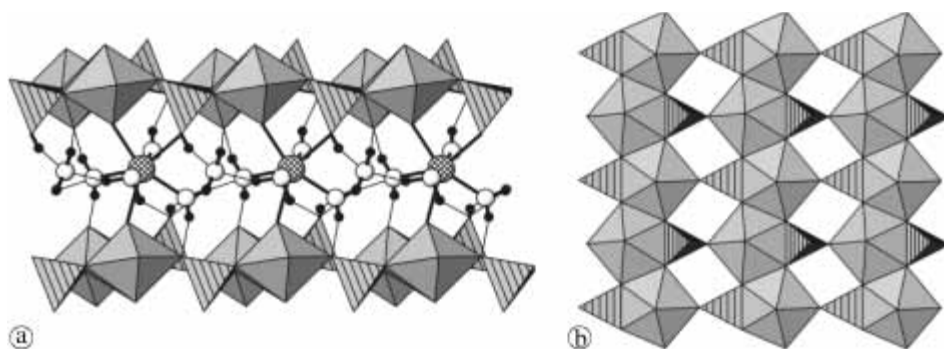


**Fig. 1.** The structure of uranophane,  $\text{Ca}(\text{UO}_2)_2(\text{SiO}_3\text{OH})_2(\text{H}_2\text{O})_5$ . The structure is based upon sheets of uranyl pentagonal bipyramids (gray) and silicate tetrahedra (gray with parallel lines) that are linked through an interlayer containing Ca (cross-hatched) and  $\text{H}_2\text{O}$  (O atoms are white, H atoms are solid circles).

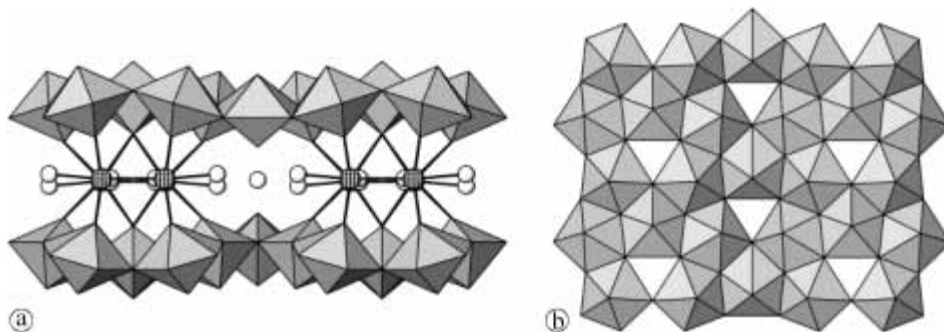


**Fig. 2.** The structure of Na-compreignacite,  $\text{Na}_2[(\text{UO}_2)_3\text{O}_2(\text{OH})_3]_2(\text{H}_2\text{O})_7$ . The structure contains sheets of uranyl pentagonal bipyramids (b) that are linked by bonds to interlayer Na (cross-hatched) and  $\text{H}_2\text{O}$  (white).

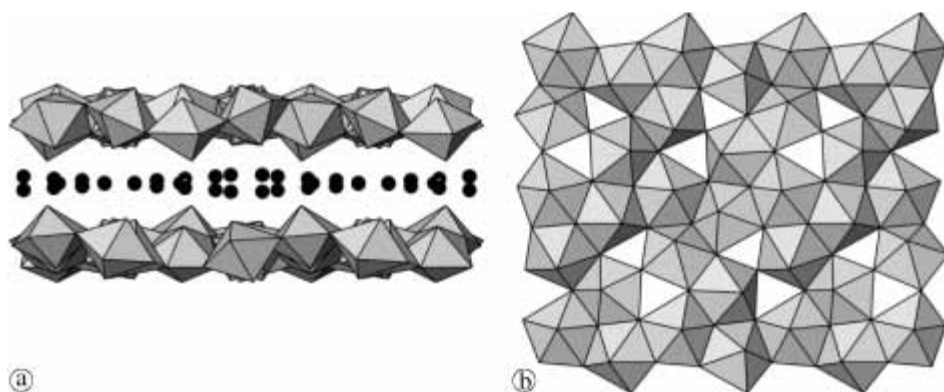


**Fig. 3.** The structure of meta-schoepite,  $\text{UO}_3 \cdot 2\text{H}_2\text{O}$ . The structure is based upon sheets of uranyl pentagonal bipyramids (b) that are linked by hydrogen bonds to interlayer  $\text{H}_2\text{O}$  groups (black).

isostructural with compreignacite. The structure of compreignacite [26] contains  $\alpha\text{-U}_3\text{O}_8$ -type sheets of edge and vertex-sharing uranyl pentagonal bipyramids, with monovalent cations and  $\text{H}_2\text{O}$  groups in the interlayer (Fig. 2a). The  $\alpha\text{-U}_3\text{O}_8$ -type sheet (Fig. 2b) is common in the structures of uranyl oxide hydrates, and is compatible with a variety of hydroxyl distributions within the sheet, as well as a range of interlayer configurations. The sheets in compreignacite are connected both by bonds to the interlayer cations, and through a complex network of H bonding.

### 4.3 Meta-schoepite

The structure of meta-schoepite (Fig. 3a) [27] involves electroneutral sheets of edge and vertex-sharing uranyl pentagonal bipyramids (Fig. 3b), with  $\text{H}_2\text{O}$  groups located in the interlayer. The sheets are connected only through H bonding to the interlayer  $\text{H}_2\text{O}$  groups. The sheet found in meta-schoepite is compatible with a variety of interlayer configurations; topologically identical sheets of uranyl polyhedra also occur in schoepite [28] and the Pb uranyl oxide hydrate fourmarierite [29].

### 4.4 $\beta\text{-UO}_2(\text{OH})_2$

The compound  $\beta\text{-UO}_2(\text{OH})_2$  is not known as a mineral, but is readily synthesized under mild hydrothermal conditions at  $\text{pH} \sim 4$ . Its structure [30] contains  $(\text{UO}_2)^{2+}$  uranyl ions that are coordinated by four OH groups arranged at the equatorial vertices of square bipyramids. Sheets are formed by the sharing of equatorial vertices between the square bipyramids (Fig. 4a). Adjacent sheets are linked only through H bonds that extend from OH groups of one sheet to  $\text{O}_{\text{ur}}$  atoms of adjacent sheets; the structure does not contain any interlayer constituents (Fig. 4b).

## 5. Crystal chemistry of $\text{Np}^{5+}$

Under the conditions present where  $\text{UO}_2$  spent nuclear fuel is altering to uranyl compounds,  $\text{Np}^{5+}$  is likely to be the dominant oxidation state of Np [31]. Eleven crystal structures have been considered that contain  $\text{Np}^{5+}$  (Table 1). Each contains an approximately linear neptunyl ion,  $\text{NpO}_2^+$ . In most cases the neptunyl ion is coordinated by five ligands arranged at the equatorial vertices of pentagonal bipyramids

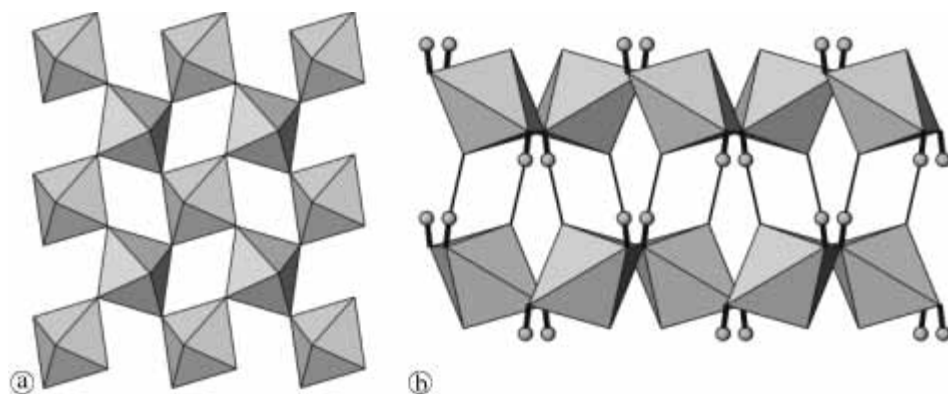


**Fig. 4.** The structure of  $\beta$ -( $\text{UO}_2$ )( $\text{OH}$ ) $_2$ . The structure consists of sheets of uranyl square bipyramids (a) that are linked by H bonds (b).

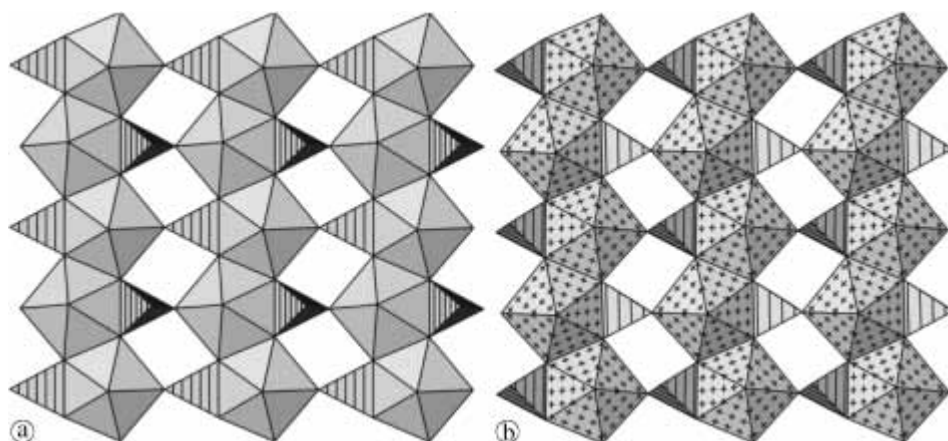


**Fig. 5.** Comparison of the uranyl silicate sheet in uranophane (a) with the neptunyl chromate sheet in  $\text{Cs}(\text{NpO}_2)(\text{CrO}_4)(\text{H}_2\text{O})$  [37]. (b) Note that the topologies of these sheets are identical.

**Table 1.**  $\text{Np}^{5+}$ –O bond lengths ( $\text{\AA}$ ) in inorganic compounds.

	Neptunyl		Equatorial				Reference	
$\text{Cs}_3\text{NpO}_2(\text{SO}_4)_2(\text{H}_2\text{O})_2$	1.82	1.82	2.39	2.39	2.52	2.46	2.59	[32]
$\text{K}_4(\text{H}_5\text{O}_2)(\text{NpO}_2)_3(\text{MoO}_4)_4(\text{H}_2\text{O})_4$	1.84	1.84	2.39	2.39	2.39	2.39	2.39	[33]
	1.90	1.85	2.41	2.44	2.43	2.41	2.45	
$(\text{Co}(\text{NH}_3)_6)\text{H}_8\text{O}_3(\text{NpO}_2)(\text{SO}_4)_3$	1.84	1.81	2.56	2.52	2.42	2.47	2.40	[34]
$(\text{NpO}_2)_2(\text{NO}_3)_2(\text{H}_2\text{O})_5$	1.85	1.83	2.48	2.42	2.59	2.60	2.60	2.64 [35]
	1.84	1.84	2.42	2.50	2.50	2.46	2.45	
$(\text{Co}(\text{NH}_3)_6)((\text{H}_2\text{O})\text{NpO}_2(\text{SeO}_4)_2)(\text{H}_2\text{O})_2$	1.85	1.85	2.46	2.46	2.43	2.43	2.49	[36]
$\text{Cs}(\text{NpO}_2)(\text{CrO}_4)(\text{H}_2\text{O})$	1.82	1.81	2.46	2.52	2.46	2.40	2.55	[37]
$(\text{NH}_4)_4(\text{NpO}_2)_2(\text{CrO}_4)_3$	1.85	1.83	2.46	2.59	2.40	2.43	2.43	[37]
	1.84	1.84	2.51	2.39	2.40	2.46	2.56	
$\text{Na}_2((\text{NpO}_2)_2(\text{MoO}_4)_2(\text{H}_2\text{O}))(\text{H}_2\text{O})$	1.82	1.82	2.54	2.52	2.43	2.44	2.51	[38]
	1.83	1.88	2.39	2.45	2.44	2.46		
$(\text{NpO}_2)(\text{ClO}_4)(\text{H}_2\text{O})_4$	1.77	1.82	2.50	2.47	2.45	2.43	2.34	[39]
$\text{Cs}(\text{NpO}_2)(\text{CrO}_4)(\text{H}_2\text{O})(\text{H}_2\text{O})$	1.84	1.84	2.48	2.36	2.54	2.43	2.45	[40]
$\text{K}_3(\text{NpO}_2)(\text{MoO}_4)_2$	1.83	1.85	2.49	2.46	2.43	2.42	2.49	[41]

that are capped by the O atoms of the neptunyl ion. The structural connectivity exhibited by  $\text{Np}^{5+}$  compounds bears resemblance to uranyl compounds. For example, the uranyl silicate sheets of uranophane are topologically identical to the neptunyl chromate sheets in  $\text{Cs}[(\text{NpO}_2)(\text{CrO}_4)](\text{H}_2\text{O})$  (Fig. 5).

Substitution at cationic sites in crystal structures occurs most readily when the substituting cations have similar ideal ionic radii. The average  $\text{U}-\text{O}_{\text{Ur}}$  and  $\text{U}-\text{O}_{\text{eq}}$  (eq: equatorial) bonds in uranyl pentagonal bipyramids from many well-refined structures are 1.79(4) and 2.37(9)  $\text{\AA}$ , respectively [22]. Comparable averages for  $\text{Np}^{5+}$  from 12 pentagonal bipyramids in 11 structures (Table 1) are 1.83(2)

and 2.46(5)  $\text{\AA}$ . The similarity of these bond distances implies that substitution of  $\text{Np}^{5+}$  for  $\text{U}^{6+}$  in crystal structures is likely, assuming that appropriate charge-balancing mechanisms exist.

## 6. Experimental methods

### 6.1 Synthesis of uranyl compounds

Synthesis procedures for uranyl compounds were first optimized in the absence of Np, but using otherwise identical conditions to the experiments that included Np. A double-containment method was used for each hydrothermal syn-

thesis experiment. Reactants were placed in 7 mL Teflon cups with threaded screw-on tops. After closure the cups were contained in 125 mL Teflon-lined Parr reaction vessels. Fifty mL of ultrapure water was added to each vessel to provide counter pressure during heating. Following heating, reaction vessels were allowed to cool to room temperature.

The  $\text{Np}^{5+}$  stock solution used for all experiments was obtained by dissolving  $\text{Np}(\text{ClO}_4)_5$  in 1 M  $\text{HClO}_4$ , with 13.75 mg  $\text{Np}^{5+}$  dissolved in 3.626 mL of solution.

Uranophane was synthesized by combining 5 mL of 0.2 M  $\text{UO}_2(\text{CH}_3\text{COO})_2 \cdot 2\text{H}_2\text{O}$  solution with 0.227 g  $\text{Na}_2\text{SiO}_3 \cdot 9\text{H}_2\text{O}$  and 0.282 g  $\text{Ca}(\text{CH}_3\text{COO})_2 \cdot \text{H}_2\text{O}$  in a 7 mL Teflon cup.  $\text{Np}^{5+}$  stock solution was added to four identical preparations to give  $\sim 10$ , 65, 135 and 350 ppm of  $\text{Np}^{5+}$  in solution. Ultrapure  $\text{H}_2\text{O}$  was added so that the sum of  $\text{Np}^{5+}$  stock solution and  $\text{H}_2\text{O}$  totaled 0.5 mL. The pH of the solutions as mixed ranged from 6.0 to 6.8; each was adjusted to 5.4 by addition of 1 M  $\text{HClO}_4$ . One mL aliquots of solution were collected for each experiment and retained for later analysis. The reactants were heated at 100 °C for 24 hours.

Na-compreignacite was obtained by combining 5 mL of 0.2 M  $\text{UO}_2(\text{CH}_3\text{COO})_2 \cdot 2\text{H}_2\text{O}$  solution with 0.041 g  $\text{Na}_2\text{CO}_3$ .  $\text{Np}^{5+}$  stock solution was added to two identical preparations to give  $\sim 200$  and 400 ppm of  $\text{Np}^{5+}$  in solution. Ultrapure  $\text{H}_2\text{O}$  was added to each so that  $\text{Np}^{5+}$  stock solution and  $\text{H}_2\text{O}$  totaled 0.5 mL. The solution pH as mixed ranged from 5.2 to 3.7; these were adjusted into the range 5.2 to 5.7 by addition of 15%  $\text{NaOH}$  solution. A 1 mL aliquot of each solution was taken and retained for later analysis. Reactants were heated to 100 °C for 24 hours.

Meta-schoepite was synthesized by combining 0.143 g  $\text{UO}_3$  powder with 5 mL of ultrapure  $\text{H}_2\text{O}$  followed by heating at 75 °C for 24 hours.  $\text{Np}^{5+}$  stock solution was added to three identical preparations to give  $\sim 20$ , 200 and 500 ppm of  $\text{Np}^{5+}$  in solution. Ultrapure  $\text{H}_2\text{O}$  was added to each so that  $\text{Np}^{5+}$  stock solution and  $\text{H}_2\text{O}$  totaled 0.5 mL. The pH of the solutions as mixed ranged from 1.7 to 4.2; each were adjusted into the range 4.0 to 4.2 by addition of 15%  $\text{NaOH}$  solution. A 1 mL aliquot of each solution was taken prior to sealing the reaction vessels.

$\beta\text{-UO}_2(\text{OH})_2$  was prepared by combining 5 mL of 0.2 M  $\text{UO}_2(\text{CH}_3\text{COO})_2 \cdot 2\text{H}_2\text{O}$  solution and 0.041 g  $\text{Na}_2\text{CO}_3$ .  $\text{Np}^{5+}$  stock solution was added to identical preparations to provide  $\sim 15$  and 425 ppm  $\text{Np}^{5+}$  in solution, and ultrapure  $\text{H}_2\text{O}$  was added to each preparation so that  $\text{Np}$  stock solution and  $\text{H}_2\text{O}$  totaled 0.5 mL. The pH of the solutions as mixed ranged from 4.4 to 4.9; these were adjusted into the range of 4.2 to 4.4 by the addition of 1 M  $\text{HClO}_4$ .

After heating solutions were sampled, and powders were recovered by filtration. The uranophane, Na-compreignacite and  $\beta\text{-UO}_2(\text{OH})_2$  products all contained crystals of Na uranyl acetate, as identified by X-ray diffraction. Each powder was washed about eight times using a total of 150 mL of boiling water, which removed all visible traces of Na uranyl acetate. Subsequently, each powder was divided into three portions; one was used for X-ray powder diffraction analysis, one was prepared for chemical analysis without further treatment, and the third was washed by shaking a combination of the powder and 2 mL 0.5 M acetic acid for 20 seconds to remove adsorbed  $\text{Np}^{5+}$ .

## 6.2 X-ray powder diffraction analysis of uranyl compounds

X-ray powder diffraction patterns were collected for each powder following washing with boiling water. Patterns were collected over the two-theta range 2–150° with a scan-rate of 0.25° per minute using an automated Scintag theta-theta diffractometer and  $\text{Cu } K_\alpha$  radiation. The diffractograms were analyzed to determine the identity and purity of the powders by comparison with patterns provided in the Powder Diffraction File.

The uranophane and meta-schoepite powders contained no detectable impurity phases. The Na-compreignacite powder included  $\sim 5\%$ – $10\%$  of  $\beta\text{-}(\text{UO}_2)(\text{OH})_2$ . The  $\beta\text{-}(\text{UO}_2)(\text{OH})_2$  powder contained no detectable impurities in the case of experiment UOH-1, and  $\sim 5\%$  Na-compreignacite in experiment UOH-2. Detection of phases present at levels below  $\sim 2\%$ , or the presence of amorphous material, is not possible using powder diffraction. Representative diffraction patterns for each phase are presented in Fig. 6.

## 6.3 Chemical analyses of uranyl compounds and solutions

Chemical analyses were done for aliquots of solutions collected prior to hydrothermal treatment, the solutions remaining after treatment, precipitates that were washed with boiling water, and precipitates that were washed using both boiling water and acetic acid.

In most cases precipitates had formed in the solutions prior to their analysis. They were acidified using a few drops of 6 M hydrochloric acid, which completely dissolved the precipitates in most cases. Solutions containing Si (the uranophane series) contained a white gel-like precipitate even after acidification. Powders for analysis were each dissolved in 5 mL of 0.6 M hydrochloric acid.

Solutions were analyzed for Ca, Na, and U by inductively coupled plasma-atomic emission spectrometry (ICP-AES) using a Perkin Elmer Optima Series Model 3300 DV instrument operated in the radial viewing mode. Calibration standards were prepared by volumetric dilution of certified solution standards procured from SCP Science, Champlain NY (Na and Ca) or Spex CertiPrep, Metuchen NJ (U). Samples were diluted as necessary to provide signals that fell with the range of the standards, which sometimes required different levels of dilution to accommodate all three elements.

$\text{Np}$  was determined by inductively coupled plasma-mass spectrometry (ICP-MS) with a VG Elemental Plasma Quad II Plus system, using Th as an internal standard. The quadrupole mass analyzer was tuned to optimize resolution at mass 237 and minimize tailing of the U-238 peak into the 237 mass position. Samples were diluted, using the U concentrations measured by ICP-AES and ICP-MS screening runs as a guide, to a concentration of 10 mg/L U or to a  $\text{Np}$  concentration lower than the highest calibration standard (40  $\mu\text{g/L}$ ). Analysis of standards containing 10 mg/L U and various amounts of added  $\text{Np}$  demonstrated that the low mass tail of the 238 peak at this U concentration made a small contribution to the  $\text{Np}$ -237 signal, which corresponded to 0.2  $\mu\text{g/L}$   $\text{Np}$ . Corrections were applied accordingly to the measured  $\text{Np}$  values in proportion to the U concentration calculated from the ICP-AES data and the

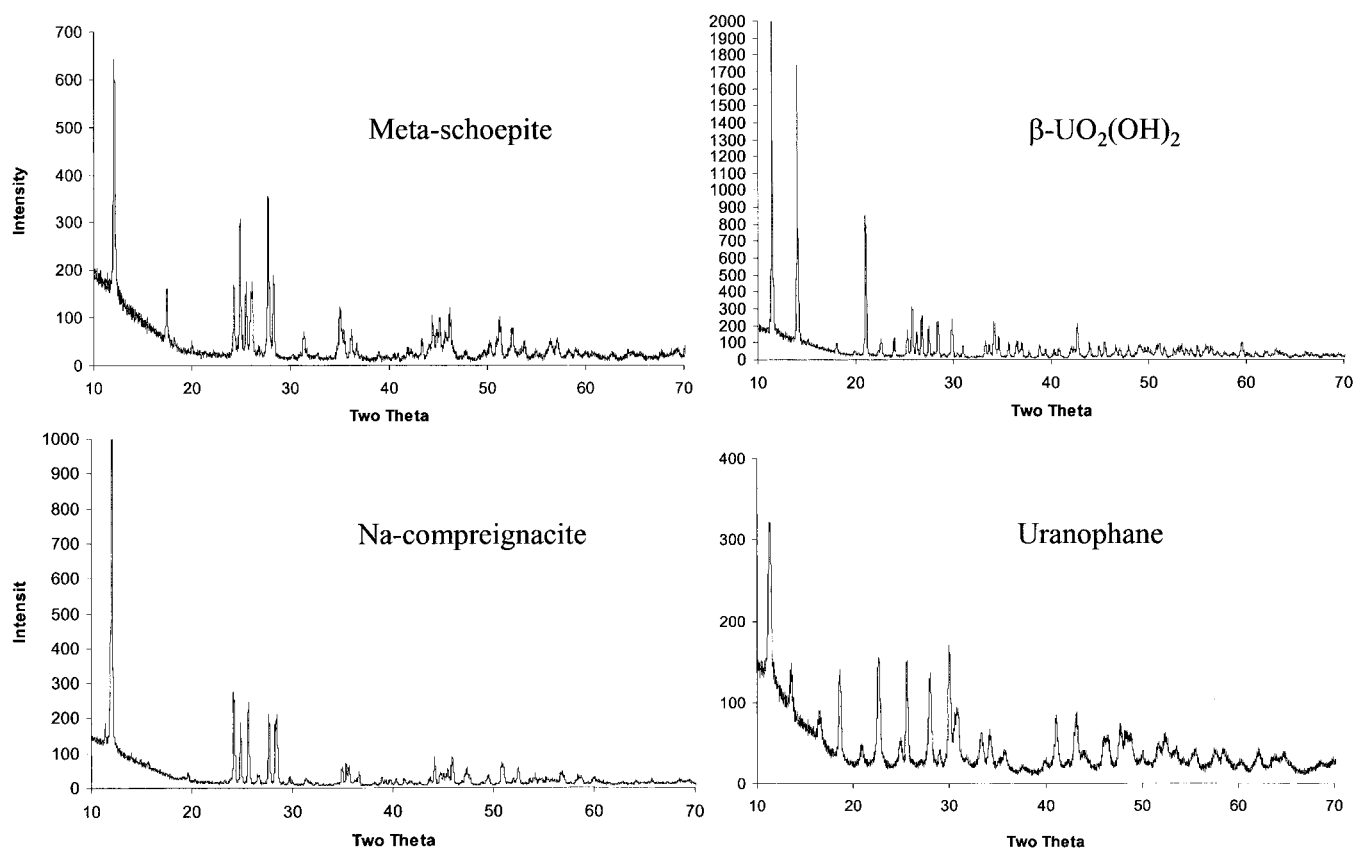


Fig. 6. Representative powder diffraction patterns for each phase studied, as collected following Np-incorporation experiments.

Table 2. Pertinent results of chemical analyses<sup>a</sup> of initial solutions and resulting powders.

	Np in initial solution (mg/mL)	Powder analyzed (mg)	Ca (wt. %)	Na (wt. %)	U (wt. %)	Np (ppm)	Np (ppm) acid washed	Np ppm of actinides
Uranophane								
UR-1	0.01	9.70	4.3	0.8	52.9	5	n.d.	10
UR-2	0.07	34.90	3.8	0.6	48.3	35	29	72
UR-3	0.14	40.53	4.0	0.4	50.4	81	54	160
UR-4	0.36	37.08	3.8	0.3	47.8	194	182	406
Theoretical			4.7		55.6			
Na Compreignacite								
NAC-1	0.20	35.63		2.7	75.1	167	133	220
NAC-2	0.43	30.15		2.9	78.4	390	411	498
Theoretical				2.3	72.9			
Meta Schoepite								
MSC-1	0.02	40.14			77.5	n.d.	n.d.	n.d.
MSC-2	0.20	36.49			77.6	19	n.d.	24
MSC-3	0.48	25.33			71.2	26	n.d.	36
Theoretical					73.9			
$\beta$ -(UO <sub>2</sub> )(OH) <sub>2</sub>								
UOH-1	0.01	12.21		0.7	77.7	n.d.	n.d.	n.d.
UOH-2	0.42	12.90		0.6	76.9	17	n.d.	22
Theoretical					78.3			

a: accuracy estimated to be within  $\pm 10\%$ ;

n.d.: not detected.

dilution applied for each ICP-MS sample. Calibration standards for Np measurements were prepared by volumetric dilution of a stock solution that was standardized by alpha counting. A measured aliquot of the stock solution was

deposited on a planchet and the total alpha emission rate was measured using a gas proportional counting system in 2- $\pi$  geometry. The energy distribution of alpha particles was analyzed using an EG&G ORTEC Model 576A Al-

pha Spectrometer with a solid-state surface-barrier detector that records the number of detected particles as a function of energy. This analysis showed that 79.8% of the emitted alpha particles were from decay of Np-237, 15.8% from Pu-238, and 4.4% from Pu-239 in the Np source material. The Np concentration in the stock solution was calculated using a specific activity for Np-237 of 1565.1 dpm per  $\mu\text{g}$  Np after accounting for the efficiency of the  $2\pi$  counter and the fraction of the alpha activity attributable to Np. The analytical results are summarized in Table 2.

Six samples representing a range of Np concentrations were analyzed in duplicate. In four cases results were identical within 5%, whereas the others differed by 13 and 15%. Samples were each diluted to  $\sim 10$  ppm U for analysis; based upon standards the detection limit for Np was determined to be 5 ppm of the U concentration in the specimen. For example, the Np detection limit for a sample containing 2000 ppm U was 0.01 ppm. Analyses that resulted in Np concentrations below detection limits are so indicated in Table 2.

## 7. Results and discussion

The analytical results presented in Table 2 are expected to be accurate within  $\sim 10\%$ . Reasonable agreement has been attained between measured and theoretical values for the major elements of each phase. For the uranophane analyses, measured values are slightly below theoretical values, whereas the Ca:U ratios range from 0.94:2 to 0.96:2, in good agreement with the theoretical ratio of 1:2, especially given that some Na may substitute for Ca in the structure. The powders of uranophane may contain unreacted amorphous silica, which would not have been detected in the X-ray diffraction analysis, and would account for the somewhat low values for Ca and U (samples were not analyzed for Si because of the difficulty of dissolving Si). The Na:U ratios for analyses of Na-compreignacite are 1.1:3, in reasonable agreement with the expected value of 1:3.

The Np content of the synthesized powder, as ppm of total actinides, is compared to the Np concentration of the

initial solution as determined by the chemical analyses in Fig. 7. Fig. 7a gives results for powders washed in boiling water, and the data in Fig. 7b is for powders that were also washed with 0.5 M acetic acid.

Powders of meta-schoepite and  $\beta\text{-(UO}_2\text{)(OH)}_2$  synthesized from solutions containing various Np concentrations contained little Np; analysis for meta-schoepite powders range from 5 to 36 ppm Np (given as Np of total actinides), whereas the corresponding range for powders of  $\beta\text{-(UO}_2\text{)(OH)}_2$  is 5 to 22 ppm. The highest levels observed in each case were for powders synthesized from solutions containing the highest concentrations of  $\text{Np}^{5+}$ . Following washing in 0.5 M acetic acid, maximum Np contents for meta-schoepite powders declined to below detection, which suggests that much of the Np was adsorbed to the surface of crystals, rather than incorporated into the crystal structure. Low yields of  $\beta\text{-UO}_2\text{(OH)}_2$  precluded analysis of acid-washed crystals for UOH-2; in UOH-1 the Np content of the powders following the acid-wash was below detection.

Powders of uranophane and Na-compreignacite washed in boiling water contain Np ranging up to 406 and 498 ppm, respectively. There is a linear relationship between the Np content of the uranophane and Na-compreignacite powders and the  $\text{Np}^{5+}$  concentration in the initial solution (Fig. 7a). Np is incorporated into the powders of uranophane and Na-compreignacite in approximately the same concentrations as present in the mother solutions. Washing the powders in 0.5 M acetic acid reduced the Np concentrations somewhat in some cases (Table 2, Fig. 7b), but the bulk of the Np was unaffected by the acid-wash, indicating that it is likely incorporated into phases present in the powders, rather than sorbed onto their surfaces.

It is possible that powders of uranophane and Na-compreignacite contain small amounts of a Np-rich phase that could not be detected by X-ray powder diffraction. It is also possible that the powders contain a Np-bearing amorphous phase that would not have been detected using X-ray diffraction. Assuming the hypothetical Np phase contained  $\sim 70$  wt. % Np, the powders would contain at most  $\sim 0.06$  wt. % of the phase, making it virtually impossible to detect by any method. However, several aspects of our

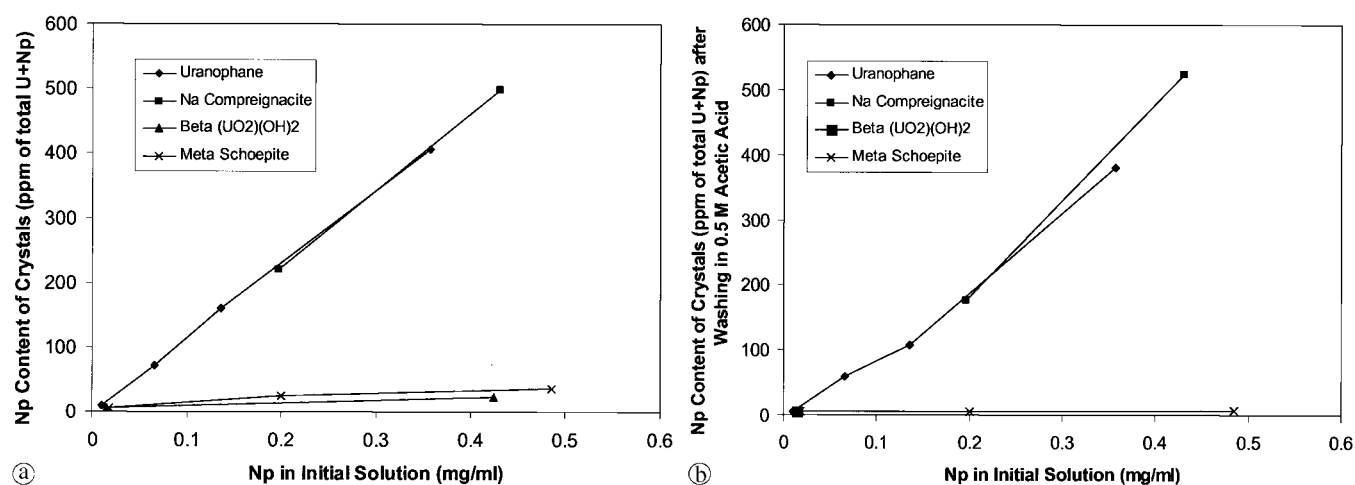


**Fig. 7.** Results of the chemical analysis of Np-substituted uranyl compounds. Comparison of the Np concentration in the initial solution (ppm) prior to the synthesis experiment with the Np content in the crystals, given as the amount of Np in ppm of the total actinides (U + Np). (a) Results for powders washed in boiling water. (b) Results for powders washed in boiling water, followed by washing with 0.5 M acetic acid.

results support incorporation of  $\text{Np}^{5+}$  into uranophane and Na-compreignacite, rather than precipitation of a Np-rich phase or inclusion in an amorphous phase. Incorporation of Np into the powders is a linear function of the concentration of  $\text{Np}^{5+}$  in the initial solution. Had a Np-rich phase precipitated in the higher-Np concentration experiments, departures from the linear trends observed would be expected. Also, the lack of Np in the powders of meta-schoepite and  $\beta\text{-(UO}_2\text{)(OH)}_2$  rules out precipitation of a Np-bearing phase in those experiments, even though the experiments contained comparable levels of Np as those for uranophane and Na-compreignacite. The synthesis experiments for Na-compreignacite and  $\beta\text{-(UO}_2\text{)(OH)}_2$  differed only in pH (5.2–5.7 versus 4.2–4.4, respectively); it seems unlikely that a Np-rich phase would precipitate in the Na-compreignacite experiment, but be absent in the  $\beta\text{-(UO}_2\text{)(OH)}_2$  powder.

The only high-valence cation present in the structures of Na-compreignacite, meta-schoepite, and  $\beta\text{-(UO}_2\text{)(OH)}_2$  is  $\text{U}^{6+}$ , whereas uranophane contains  $\text{U}^{6+}$  and  $\text{Si}^{4+}$ . It is unlikely that  $\text{Np}^{5+}$  will substitute for a low-valence cation such as Na or Ca in a crystal structure, and the coordination environment typical of  $\text{Np}^{5+}$  is highly incompatible with the tetrahedral sites of  $\text{Si}^{4+}$  in uranophane. Given the close geometrical similarity between the coordination environments observed in structures about  $\text{Np}^{5+}$  and  $\text{U}^{6+}$ , substitution of  $\text{Np}^{5+}$  for  $\text{U}^{6+}$  is the most likely mechanism for incorporation of  $\text{Np}^{5+}$  in the structures of the phases considered in this study. However, in order for  $\text{Np}^{5+}$  to replace  $\text{U}^{6+}$  in a structure, a local charge-balance mechanism must also exist.

Significant incorporation of  $\text{Np}^{5+}$  appears to have occurred in uranophane and Na-compreignacite, each of which contain sheets with net negative charges that involve uranyl pentagonal bipyramids, and interlayers with low-valence cations and  $\text{H}_2\text{O}$  groups. Meta-schoepite, which did not incorporate much  $\text{Np}^{5+}$ , contains sheets of uranyl pentagonal bipyramids, but the sheets are neutral, and the interlayer contains only  $\text{H}_2\text{O}$ . In the case of  $\beta\text{-(UO}_2\text{)(OH)}_2$ , which did not incorporate significant  $\text{Np}^{5+}$ , there are no interlayer constituents. These observations suggest that the charge-balance mechanism that may permit incorporation of  $\text{Np}^{5+}$  into uranophane and Na-compreignacite involves charged species in the interlayer.

There is considerable circumstantial evidence that the Np has been incorporated into these structures as  $\text{Np}^{5+}$ . The initial  $\text{Np}^{5+}$  stock solution contained only  $\text{Np}^{5+}$ , and the synthesis experiments were conducted within the expected stability field of this oxidation state. Had  $\text{Np}^{5+}$  been oxidized to  $\text{Np}^{6+}$ , much higher levels of incorporation would be expected, as the geometry of the  $\text{Np}^{6+}$  coordination environment is a close match to that of  $\text{U}^{6+}$ , and no charge-balance mechanism would be required. Also,  $\text{Np}^{6+}$  should have been incorporated in abundance into the structures of meta-schoepite and  $\beta\text{-(UO}_2\text{)(OH)}_2$  had it been present in the solutions.

Our results, which did not find significant  $\text{Np}^{5+}$  in powders of meta-schoepite, are not consistent with Buck *et al.* [10], who reported Np in meta-schoepite that formed as an alteration phase on spent fuel. The lack of a variety of low-valence cations in our synthesis experiments, such as K, Cs and Ca, may have precluded a charge-balance

mechanism; we intend to re-examine Np incorporation into meta-schoepite with various counter ions in the synthesis solutions.

This study provides evidence for the likely incorporation of  $\text{Np}^{5+}$  into the structures of uranophane and Na-compreignacite, phases that are expected to form due to the alteration of spent nuclear fuel in Yucca Mountain. Such incorporation could have a profound impact upon the long-term mobility of Np in the repository because Np incorporated into uranyl compounds may be immobilized for thousands of years.

Additional studies are required to determine effects of the presence of counter-ions, pH, temperature and time on Np incorporation in uranyl compounds. Studies are also needed for additional uranyl compounds that are expected to form under Yucca Mountain conditions.

*Acknowledgment.* This research was supported by the Environmental Management Science Program of the Office of Science, U.S. Department of Energy, grant DE-FG07-97ER14820 to PCB. Research at Argonne is supported by the U.S. DOE, Basic Energy Sciences, Chemical Sciences, under contract W-31-109-ENG-38. We thank Dr. Lynne Soderholm for assisting with experiments and providing laboratory facilities for the Np experiments. The elemental analyses were provided by the Analytical Chemistry Laboratory, Chemical Technology Division, Argonne National Laboratory, under supervision of Donald G. Graczyk. Measurements were done by Susan Lopykinski (ICP-AES) and Florence Smith (ICP-MS). Delbert Bowers prepared the Np standard stock solution and did the alpha-counting measurements. We thank Robert Finch for comments on an earlier version of the manuscript.

## References

1. Finch, R. J., Ewing, R. C.: *J. Nucl. Mater.* **190**, 133 (1992).
2. Percy, E. C., Prikryl, J. D., Murphy M. W., Leslie, B. W.: *Appl. Geochem.* **9**, 713 (1994).
3. Wronkiewicz, D. J., Bates, J. K., Gerding, T. J., Veleckis, E., Tani, B. S.: *J. Nucl. Mater.* **190**, 107 (1992).
4. Wronkiewicz, D. J., Bates, J. K., Wolf, S. F., Buck, E. C.: *J. Nucl. Mater.* **238**, 78 (1996).
5. Finch, R. J., Buck, E. C., Finn, P. A., Bates, J. K.: Oxidative corrosion of spent  $\text{UO}_2$  fuel in vapor and dripping groundwater at 90 °C. In: *Scientific Basis for Nuclear Waste Management XXII*. (Wronkiewicz, D. J., Lee, J. H., eds.) Mater. Res. Soc. Symp. Proc. **556**, 431 (1999).
6. Finn, P. A., Hoh, J. C., Wolf, S. F., Slater, S. A., Bates, J. K.: *Radiochim. Acta* **74**, 65 (1996).
7. Finn, P. A., Wolf, S. F., Leonard, R. A., Finch, R. J., Buck, E. C.: Presented at the seventh international conference on the Chemistry and Migration Behavior of Actinides and Fission Products in the Geosphere, Incline Village, Lake Tahoe, Nevada, USA, September 26–October 1, 1999, Abstracts Vol. **7**, 17 (1999).
8. Buck, E. C., Wronkiewicz, D. J., Finn, P. A., Bates, J. K.: *J. Nucl. Mater.* **249**, 70 (1997).
9. Finch, R. J., Suksi, J., Rasilainen, K., Ewing, R. C.: U-series ages of secondary uranium minerals with applications to the long-term evolution of spent nuclear fuel. In: *Scientific Basis for Nuclear Waste Management XIX*. (Murphy, W. M., Knecht, D. A., eds.) Mater. Res. Soc. Symp. Proc. **412**, 823 (1996).
10. Buck, E. C., Finch, R. J., Finn, P. A., Bates, J. K.: Retention of neptunium in uranyl alteration phases formed during spent fuel corrosion. In: *Scientific Basis for Nuclear Waste Management XXI*. (McKinley, I. G., McCombie, C. H., eds.) Mater. Res. Soc. Symp. Proc. **506**, 87 (1998).
11. Burns, P. C.: *J. Nucl. Mater.* **265**, 218 (1999).
12. Burns, P. C., Ewing, R. C., Miller, M. L.: *J. Nucl. Mater.* **245**, 1 (1997).
13. Burns, P. C., Hill, F. C.: *Can. Mineral.* **38**, 175 (2000).

14. Burns, P. C., Olson, R. A., Finch, R. J., Hanchar, J. M., Thibault, Y. J.: *J. Nucl. Mater.* **278**, 290 (2000).
15. Chen, F., Burns, P. C., Ewing, R. C.: *J. Nucl. Mater.* **278**, 225 (2000).
16. Chen, F., Burns, P. C., Ewing, R. C.: *79Se: J. Nucl. Mater.* **275**, 81 (1999).
17. Cahill, C. L., Burns, P. C.: *Am. Mineral.* **85**, 1294 (2000).
18. Burns, P. C., Li, Y.: *Am. Mineral.* **87**, 550 (2002).
19. Whipple, C. G., Witherspoon, P. A., Budnitz, R. J., Ewing, R. C., Moeller, D. W., Payer, J. H.: Final report of the Total System Performance Assessment (TSPA) Peer Review Panel (1999).
20. Frondel, C.: Systematic mineralogy of uranium and thorium. U.S. Geological Survey Bulletin (1958) p. 1064.
21. Finch, R. J., Murakami, T.: Systematics and paragenesis of uranium minerals. In: *Uranium: Mineralogy, Geochemistry and the Environment*. (Burns, P. C., Finch, R. J., eds.) *Rev. Mineral.* **38**, 91 (1999).
22. Burns, P. C., Ewing, R. C., Hawthorne, F. C.: *Can. Mineral.* **35**, 1551 (1997).
23. Burns, P. C., Miller, M. L., Ewing, R. C.: *Can. Mineral.* **34**, 845 (1996).
24. Burns, P. C.: The crystal chemistry of uranium. In: *Uranium: Mineralogy, Geochemistry and the Environment*. (Burns, P. C., Finch, R. J., eds.) *Rev. Mineral.* **38**, 23 (1999).
25. Ginderow, D.: *Acta Crystallogr. C* **44**, 421 (1988).
26. Burns, P. C.: *Can. Mineral.* **36**, 1061 (1998).
27. Weller, M. T., Light, M. E., Gelbrich, T.: *Acta Crystallogr.* **56**, 577 (2000).
28. Finch, R. J., Cooper, M. A., Hawthorne, F. C., Ewing, R. C.: *Can. Mineral.* **34**, 1071 (1996).
29. Li, Y., Burns, P. C.: *Can. Mineral.* **38**, 737 (2000).
30. Taylor, J. C., Bannister, M. J.: *Acta Crystallogr.* **28**, 2995 (1972).
31. Nitsche, H., Roberts, K., Beacraft, K., Prussin, T., Keeney, D., Carpenter, S. A., Hobart, D. E.: Solubility and Speciation Results from Over and Undersaturation Experiments on Neptunium, Plutonium, and Americium in Water from Yucca Mountain Region Well UE-25p #1. Los Alamos National Laboratory report LA-13017-MS (November 1995).
32. Grigor'ev, M. S., Yanovskii, A. I., Fedoseev, A. M., Budantseva, N. A., Struchkov, Yu. Y., Krot, N. N.: *Soviet Radiochem.* **33**, 118 (1991).
33. Grigor'ev, M. S., Charushnikova, I. A., Fedoseev, A. M., Budantseva, N. A., Baturin, N. A., Regel, L. L.: *Radiokhimiya* **33**, 19 (1991).
34. Grigor'ev, M. S., Fedoseev, A. M., Budantseva, N. A., Yanovskii, A. I., Struchov, Y. T., Krot, N. N.: *Soviet Radiochem.* **33**, 252 (1991).
35. Grigor'ev, M. S., Charushnikova, I. A., Krot, N. N., Yanovskii, A. I., Struchkov, Yu. Y.: *Zhurnal Neorganicheskoi Khimii* **39**, 179 (1994).
36. Grigor'ev, M. S., Plotnikova, T. E., Budantseva, N. A., Fedoseev, A. M., Yanovskii, A. I., Struchkov, Yu. Y.: *Radiokhimiya* **34**, 1 (1992).
37. Grigor'ev, M. S., Baturin, N. A., Fedoseev, A. M., Budantseva, N. A.: *Soviet Radiochem.* **33**, 504 (1991).
38. Grigor'ev, M. S., Baturin, N. A., Fedoseev, A. M., Budantseva, N. A.: *Koordinatsionnaya Khimiya* **20**, 552 (1994).
39. Grigor'ev, M. S., Baturin, N. A., Bessonov, A. A., Krot, N. N.: *Radiokhimiya* **37**, 15 (1995).
40. Grigor'ev, M. S., Plotnikova, T. E., Baturin, N. A., Budantseva, N. A., Fedoseev, A. M.: *Radiokhimiya* **37**, 102 (1995).
41. Grigor'ev, M. S., Charushnikova, I. A., Fedoseev, A. M., Budantseva, N. A., Yanovskii, A. I., Struchkov, Y. T.: *Soviet Radiochem.* **34**, 523 (1992).